Trigonal Crystals

$$f_A=[c_{66}]^{-3}+[\tfrac{1}{2}(c_{44}+c_{11})+\tfrac{1}{2}\{(c_{44}-c_{11})^2+4c_{14}^2\}^{\frac{1}{2}}]^{-3}+[\tfrac{1}{2}(c_{44}+c_{11})-\tfrac{1}{2}\{(c_{44}-c_{11})^2+4c_{14}^2\}^{\frac{1}{2}}]^{-3}. \quad (13.1)$$

$$f_B=2[c_{44}]^{-3}+[c_{33}]^{-3}. \quad (13.2)$$

$$f_C=[\tfrac{1}{2}(c_{66}+c_{44}-2c_{14})]^{-3}+[\tfrac{1}{4}(c_{11}+2c_{44}+2c_{14}+c_{33})+\tfrac{1}{4}\{(c_{11}+2c_{14}-c_{33})^2+4(c_{14}+c_{13}+c_{44})^2\}^{\frac{1}{2}}]^{-3} + [\tfrac{1}{4}(c_{11}+2c_{44}+2c_{14}+c_{33})-\tfrac{1}{4}\{(c_{11}+2c_{14}-c_{33})^2+4(c_{14}+c_{13}+c_{44})^2\}^{\frac{1}{2}}]^{-3}. \quad (13.3)$$

$$f_D=[\tfrac{1}{5}(4c_{66}+c_{44}-4c_{14})]^{-3}+[\tfrac{1}{10}(4c_{11}+4c_{14}+5c_{44}+c_{33})+\tfrac{1}{10}\{(4c_{11}+4c_{15}-3c_{44}-c_{33})^2+4(4c_{14}+2c_{13}+2c_{44})^2\}^{\frac{1}{2}}]^{-3} + [\tfrac{1}{10}(4c_{11}+4c_{14}+5c_{44}+c_{33})-\tfrac{1}{10}\{(4c_{11}+4c_{14}-3c_{44}-c_{33})^2+4(4c_{14}+2c_{13}+2c_{44})^2\}^{\frac{1}{2}}]^{-3}. \quad (13.4)$$

$$f_G=f_C \text{ (with the sign of } c_{14} \text{ changed)}. \quad (13.5)$$

$$f_H=f_D \text{ (with the sign of } c_{14} \text{ changed)}. \quad (13.6)$$

$$f_K=\sum_{i=1}^{3} y_i^{-3}, \quad (13.7)$$

where the y_i are solutions of the equation

$$\begin{vmatrix} (4c_{66}+c_{44})/5-y & -4c_{14}/5 & -4c_{14}/5 \\ -4c_{14}/5 & (4c_{11}+c_{44})/5-y & (2c_{13}+2c_{44})/5 \\ -4c_{14}/5 & (2c_{13}+2c_{44})/5 & (4c_{44}+c_{33})/5-y \end{vmatrix}=0.$$

PHYSICAL REVIEW VOLUME 104, NUMBER 1 OCTOBER 1, 1956

Surface Conductance and the Field Effect on Germanium*

J. BARDEEN, R. E. COOVERT, S. R. MORRISON, J. R. SCHRIEFFER, AND R. SUN
Electrical Engineering Research Laboratory, University of Illinois, Urbana, Illinois

(Received April 23, 1956)

Measurements of the steady-state surface conductance and the change in this conductance with transverse electric field (field effect) have been made on a free germanium surface as a function of the gaseous ambient. The results can be understood in terms of two sets of surface states: one dependent upon the gaseous ambient and with a large density and long time constants, probably located at the outer surface of an oxide layer, and the other a set with much smaller density but shorter time constants, probably located at the germanium-germanium oxide interface. The interface states consist of a discrete state with free energy 0.13–0.15 ev below the intrinsic Fermi energy and density $1-3\times10^{11}$ states/cm^2, and a small continuous distribution. There is also indication of a discrete state greater than 0.13 ev above the intrinsic Fermi energy. The measurements suggest that surface scattering effects become important for large barrier layers.

I. INTRODUCTION

CONSIDERABLE progress[1–19] has been made in recent years in understanding the nature of the space-charge layer at a germanium surface and the way it varies with ambient and with surface treatment. There is good evidence that the surface barrier results from two different types of surface states with radically

* The experiments to be reported here were initiated by S.R.M. and J.B. The results were reported in part in reference 2 and more completely by Morrison, Sun, and Bardeen in a technical report, January 15, 1955 (unpublished). Because of uncertainties in the calibration of the field effect measurements, the results were only of qualitative value. The apparatus was revised by J.R.S., and further measurements made are reported by J. R. Schrieffer and J. Bardeen in a technical report, April 10, 1955 (unpublished). Further revisions in the equipment, particularly to increase the temperature stability, were made by R.E.C. The work was supported by the Office of Naval Research and by a grant from Motorola, Inc.

[1] W. H. Brattain and J. Bardeen, Bell System Tech. J. **32**, 1 (1953).
[2] J. Bardeen and S. R. Morrison, Physica **20**, 873 (1954).
[3] C. G. B. Garrett and W. H. Brattain, Phys. Rev. **99**, 376 (1955).
[4] E. N. Clarke, Phys. Rev. **91**, 756 (1953); **94**, 1420 (1954).
[5] S. R. Morrison, J. Phys. Chem. **57**, 860 (1953).
[6] W. Shockley and J. L. Pearson, Phys. Rev. **74**, 232 (1948).
[7] P. Handler, Bull. Am. Phys. Soc. Ser. II, **1**, 144 (1956).
[8] G. G. E. Low, Proc. Phys. Soc. (London) **B68**, 10 (1955).
[9] H. C. Montgomery and B. A. McLeod, Bull. Am. Phys. Soc. Ser. II, **1**, 53 (1956).
[10] J. R. Schrieffer, Phys. Rev. **94**, 1420 (1954); **97**, 641 (1955).
[11] W. L. Brown, Phys. Rev. **98**, 1565 (1955).
[12] Statz, de Mars, Davis, and Adams, Phys. Rev. **101**, 1272 (1956).
[13] de Mars, Statz, and Davis, Phys. Rev. **98**, 539 (1955).
[14] Statz, Davis, and de Mars, Phys. Rev. **98**, 540 (1955).
[15] R. H. Kingston, Phys. Rev. **98**, 1766 (1955); **93**, 346 (1954).
[16] W. L. Brown, Phys. Rev. **91**, 518 (1953).
[17] W. L. Brown, Phys. Rev. **100**, 590 (1955).
[18] W. L. Brown, Bull. Am. Phys. Soc. Ser. II, **1**, 48 (1956).
[19] H. A. Gebbie and K. Blodgett, Phys. Rev. **100**, 970 (1955).

different time constants. The *slow* states, probably located at the outer surface of a thin oxide layer, have time constants of seconds or minutes. Their density is so high that they effectively determine the position of the Fermi level at the surface after equilibrium has been established. It is possible to change these states and shift the position of the Fermi level relative to the energy bands by changing the ambient gas in contact with the surface. There is a much lower density of *fast* states, in most cases independent of ambient, and probably located at the interface between the oxide and the germanium proper. Time constants for these are of the order of a microsecond or less.[8]

The experiments to be reported here were designed to give information about the density and energy of the fast states. They involve measurements of conductance and change in conductance with transverse electric field (field effect) in different gaseous ambients. An alternating voltage (about 100 cps) was used for the field effect, such that the charge in the slow states remained substantially constant during each cycle while the fast states had time to come to equilibrium.

The magnitude of the surface potential, defined as the variation of the electrostatic potential at the surface from its bulk value, can be obtained by correlating the observed surface conductivity with its value given by theoretical considerations.[10] Information directly related to the energy spectrum of the fast states can then be deduced from the relation between the theoretical and experimental results of the field effect. We define the field effect mobility, $\mu_{\text{F.E.}}$, as the negative of the change in surface conductivity divided by the charge induced in the sample by the transverse field. The dependence of $\mu_{\text{F.E.}}$ upon the surface potential, ψ_s, is used to find the variation of charge trapped in surface states with ψ_s, and thus with the relative position of the Fermi level.

Somewhat different methods have been used by Statz, Davis, and de Mars[12–14] and by Brown[16] to get information about the fast states. Brown[12] also studied the field effect, but used much larger fields applied through a thin dielectric spacer. He was able to swing the bands up and down appreciably by the field alone. We depended on changes in ambient gas to get different surface potentials; the transverse field was always sufficiently small to be in the linear range. Statz *et al.* made use of the channel effect in a *pnp* transistor structure. The surface was treated so as to produce a stable *p*-type inversion layer at the surface of the *n* region. Information about the fast surface states was obtained from the variation of channel conductance with voltage applied between the channel and the *n*-type base layer. When a step voltage is applied, there is a sudden change in conductance, with the fast states reaching a new equilibrium quickly, and then the channel conductance changes slowly as the slow states attain equilibrium. Statz *et al.* found that they could account for their results with a single trapping level located about 0.155 ev below midgap. Our results are in approximate agreement with those of Statz *et al.*, but differ from those of Brown.

II. EXPERIMENTAL APPARATUS

The circuit used in the early measurements[5] of surface conductance, $\Delta\sigma$, field effect mobility, $\mu_{\text{F.E.}}$, and change in contact potential with light, $(\Delta\text{c.p.})_L$, is shown in Fig. 4, reference 2. The sample was cut so that one portion was thin ($\sim$0.015 cm) and the rest thick ($\sim$0.5 cm). The conductance and field effect were measured on the thin portion and $(\Delta\text{c.p.})_L$ and thermal drift in bulk conductivity were measured on the thick portion. The measurement of $(\Delta\text{c.p.})_L$ was made by a technique similar to that of Brattain.[1] The sample was illuminated with white light chopped at 170 cps. The light passed through the reference electrode, a perforated sheet of platinum adjacent to the sample. The change in contact potential then appeared as a 170-cps voltage between the germanium and the platinum probe. Observations of $(\Delta\text{c.p.})_L$ with changes in ambient gas confirmed that we were getting changes similar to those of Brattain. The field effect was measured using a 60-cps voltage applied to a copper sheet placed

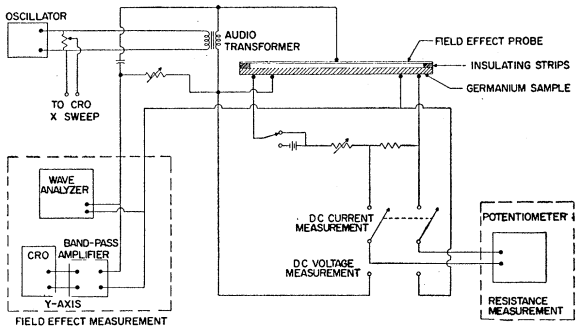

FIG. 1. Schematic diagram of the apparatus, showing how the field effect probe is mounted.

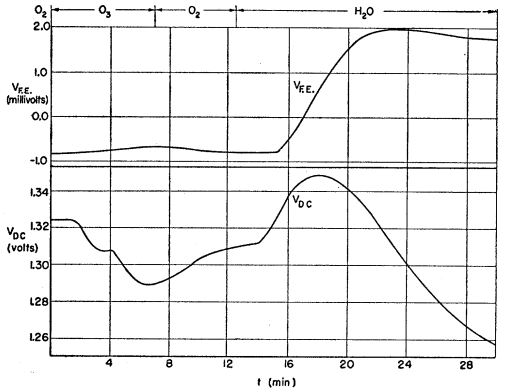

FIG. 2. Field effect voltage and dc voltage as a function of time for a 40-ohm-cm *n*-type germanium sample.

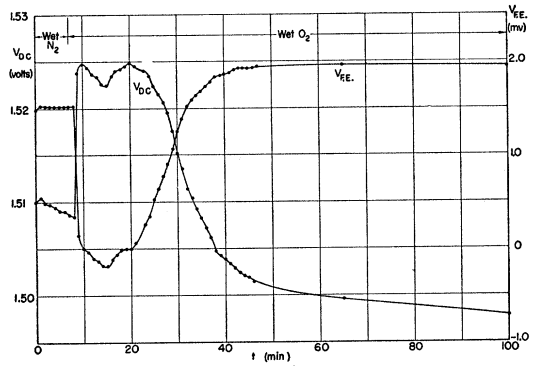

FIG. 3. Field effect voltage and dc voltage as a function of time for a 17-ohm-cm n-type germanium sample.

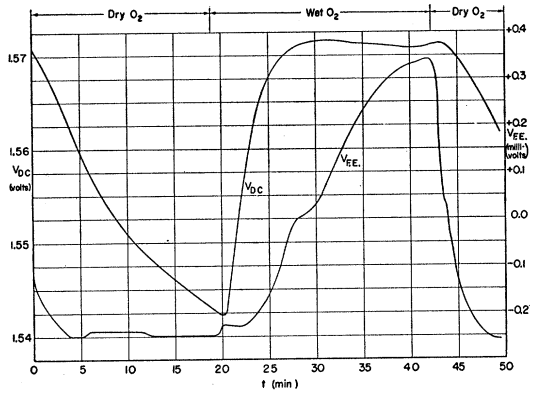

FIG. 4. Field effect voltage and dc voltage as a function of time for a run on a 17-ohm-cm n-type germanium specimen.

adjacent to the surface. The data shown in Figs. 5 and 6 of reference 2 were obtained in this way. In later work, $(\Delta c.p.)_L$ was not measured. Incorporation of a thermal bath led to dispensing with the thick portion of the sample, and facilities for measuring $(\Delta c.p.)_L$ were not included in the new apparatus. The field effect circuit was modified and a bridge (shown in Fig. 1) was used to balance out the charging current signal. A General Radio wave analyzer served to reduce stray signals and the field effect frequency was changed to 90 cps. No change in the field effect was observed for frequencies between 60 and 150 cps.[9] The pickup on the 40-ohm-cm samples was generally about 10 microvolts, allowing accurate determination of the field effect signal, which was usually an order of magnitude larger.

Water vapor, dry oxygen, ozone, nitrogen, and dry ammonia were used as gaseous ambients. A slow flow rate was used so that a detailed description of the effects could be given.

The samples were prepared by sandblasting the contact areas and attaching nickel leads with doped tin solder. The slab was then mounted on a Lucite holder which was notched suitably to accept the leads and the slab hand ground to the desired dimensions. After CP-4 etching, the samples were dried in vacuum and then maintained in dry O_2.

III. EXPERIMENTAL RESULTS

The results of the earlier runs on a 17-ohm-cm n-type thick-thin sample are shown in Fig. 5 of reference 2. It was found that the absolute height of the barrier could be obtained if the surface was swung through the conductance minimum, since the barrier height at this minimum is known from theory for a uniform surface.[10] Theory also predicts that the conductance minimum and change of sign of the field effect should occur simultaneously for a uniform surface and this condition was generally observed. The qualitative behavior of $(\Delta c.p.)_L$ was the same as observed by Brattain and Bardeen[1] upon introducing various ambients.

Figure 2 shows a typical run on a 40-ohm-cm n-type sample. These data were obtained with the modified equipment described above. It is interesting to note that $\mu_{F.E.}$ decreases upon introduction of O_3 while the conductance increases, giving evidence for reduced hole mobility due to surface scattering.[10] The same is true of the n type for $t=28$. Large changes in surface potential were obtained for these high-resistivity samples, of the order of 0.3 v. This swing is of the order of the change in contact potential observed by Brattain and Bardeen, indicating that most of the change in contact potential results from changes in the surface barrier.

Later results on a 17-ohm-cm n-type sample, shown in Fig. 3 give an exact determination of $\mu_{F.E.}$. An expansion of scale indicates a decrease of $\mu_{F.E.}$ for t greater than 60 min, another indication of surface scattering effects. The conductance minimum and change in sign of $\mu_{F.E.}$ occur simultaneously and there is a unique relationship between $\mu_{F.E.}$ and surface conductance throughout the run, indicating the surface potential is uniform over the surface. This condition was not always observed and in several runs the magnitude of the surface conductance at the conductance minima did not agree with each other. Part of this variation could be due to temperature fluctuations of the bulk resistivity; however, it is felt that the majority of the effect was due to the surface potential changing nonuniformly over the surface.

Another 17-ohm-cm n-type run shown in Fig. 4 exhibits a large p-type inversion layer existing in dry O_2. Analysis of the conductance shows that the energy bands at the surface were displaced 0.2 ev above the flat band condition, and surface scattering was undoubtedly important.

IV. ANALYSIS OF RESULTS

A theoretical plot of surface conductance including surface scattering effects is given for 17-ohm-cm and 40-ohm-cm n-type Ge in Fig. 5. The masses of both holes and electrons were taken as $0.25m_e$, the effective

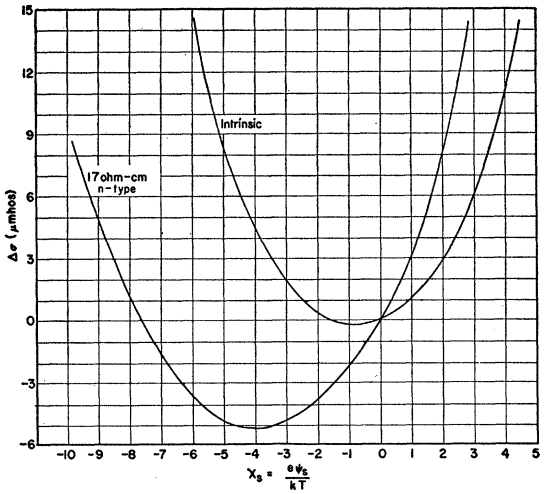

FIG. 5. The change in surface conductivity as a function of surface potential. Curves are plotted for intrinsic and 17-ohm-cm n-type material.

electron mass estimated from a calculation of Mattis and Ham[20] on conductance in thin Ge films using a model of spheroidal energy surfaces. The surface potential was determined experimentally from $\Delta\sigma$ by considering the variation of sample conductance from its value at the conductance minimum and using the curves in Fig. 5 to find the corresponding surface potential. Also, $\mu_{F.E.}$ is simply related to the field effect voltage, and hence $\mu_{F.E.}$ can be plotted as a function of surface potential.[10]

Figure 6 shows the theoretical and experimental curves of $\mu_{F.E.}$ as a function of surface potential for several runs on 40-ohm-cm n-type samples similar to Fig. 2. If surface scattering were not taken into account the theoretical curve would be asymptotic to 1 for large positive surface potential and -0.47 for large negative values. The experimental curves have been adjusted slightly to change sign at the correct surface potential. The experimental points fall considerably below the theoretical curve indicating appreciable surface shielding effects.

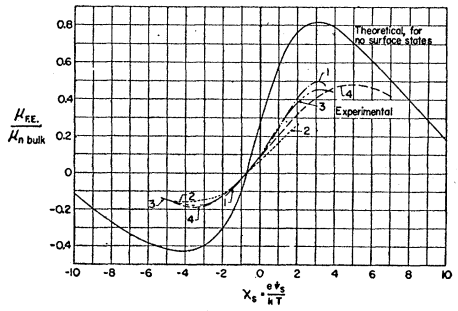

FIG. 6. Experimental and theoretical values of the field effect mobility as a function of surface potential for several runs with 40-ohm-cm n-type germanium. The theoretical curve is calculated without assuming shielding by surface states. From the difference between the theoretical and experimental curves, the density of surface states can be determined.

[20] F. Ham and D. Mattis (to be published).

Since the theoretical curve does not include effects of surface states, information about the density of the surface states can be obtained as follows. The field effect mobility is defined as

$$\mu_{F.E.} \equiv \frac{d\Delta\sigma}{dQ} = -\frac{d\Delta\sigma}{d(q_{sp}+q_s)}, \tag{1}$$

where $\Delta\sigma$ is the surface conductance per square, Q the charge on the field probe, q_{sp} the total charge in the space charge layer and q_s the charge associated with the surface states, all charges taken per square cm. Now,

$$\mu_{F.E.}(\text{theoretical}) = -\frac{d\Delta\sigma}{dq_{sp}}, \tag{2}$$

and

$$R = \frac{\mu_{F.E.}(\text{theoretical})}{\mu_{F.E.}(\text{experimental})} = 1 + \frac{dq_s}{dq_{sp}}, \tag{3}$$

or

$$dq_s = (R-1)dq_{sp}. \tag{4}$$

The change in q_{sp} with ψ_s is readily obtained by integrating Poisson's equation and is found to be

$$\frac{dq_{sp}}{d\chi_s} = \left[\frac{\kappa kT}{8\pi}\right]^{\frac{1}{2}} \frac{[(N_a-N_d)+n_0e^{\chi_s}-p_0e^{-\chi_s}]}{[(N_a-N_d)\chi_s+p_0(e^{-\chi_s}-1)+n_0(e^{\chi_s}-1)]^{\frac{1}{2}}}, \tag{5}$$

where n_0 and p_0 are the bulk carrier concentrations and $\chi_s = e\psi_s/kT$. Thus, from Eqs. (4) and (5), we have

$$\Delta q_s = \int_{\chi_{s1}}^{\chi_{s2}} (R-1)(dq_{sp}/d\chi_s)d\chi_s.$$

For intrinsic material this reduces to

$$\frac{\Delta q_s}{e} = \left(\frac{\kappa kT n_i}{2\pi e^2}\right)^{\frac{1}{2}} \int_{\chi_{s1}}^{\chi_{s2}} (R-1)\cosh(\chi_s/2)d\chi_s.$$

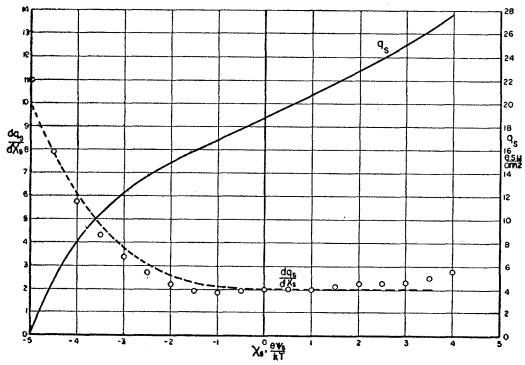

FIG. 7. Rate of change of charge in surface states with surface potential, and the surface state charge, as determined from Fig. 6.

Figure 7 shows the occupation of the traps as a function of χ_s for the 40-ohm-cm n-type material. The rapid change of $dq/d\chi_s$ in the vicinity of $-5kT$ suggests that a trap is located near this free energy. In the following, we use the ordinary Fermi function to describe the occupancy of the states, and we include the entropy term by specifying the free energy of the state. Thus for two states which are spin degenerate, the free energy would be $E_t - kT \ln 2$. Statz *et al.*[14] have observed a discrete trap located 0.155 ev below the midgap in germanium of density 0.7–1.2×10^{11} cm^{-2}. The dotted curve of Fig. 7 shows that $dq_s/d\chi_s$ derived from a density of 10^{11} cm^{-2} located at this energy agrees quite well in this region if a small continuous density is superimposed. There is also an indication of a trap located greater than $5kT$ above the mid-gap; however, it was impossible to depress the bands sufficiently to investigate this level in detail. Several runs on a different 40-ohm-cm specimen suggested a trap located 0.13 ev below midgap, of density 10^{11} cm^{-2}.

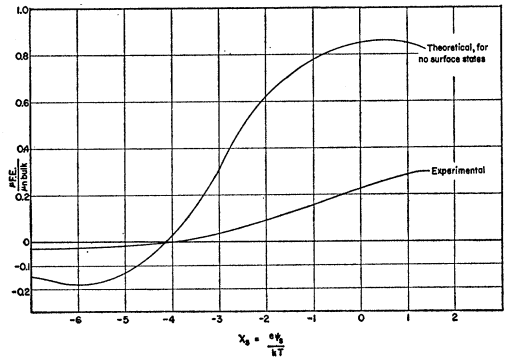

FIG. 8. Experimental and theoretical values of the field effect mobility as a function of surface potential for a typical run with a 17-ohm-cm n-type germanium specimen. The theoretical curve is calculated under the assumption of no shielding by surface states.

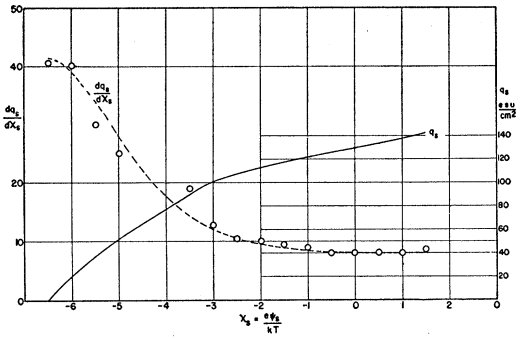

FIG. 9. Rate of change of surface states charge with surface potential, and the surface state charge, as determined from Fig. 8.

Corresponding curves for the 17 ohm-cm samples are shown in Figs. 8 and 9. Again a rapid rise in $dq/d\chi_s$ is observed; however, χ_s must be about $1.5kT$ more negative than the corresponding value for the high-resistivity sample in order to have the same proposed trap effective, because of the shift of the bulk Fermi level. A density of interface states several times larger than that derived from the high resistivity material is required to explain the 17-ohm-cm data. The dotted curve in Fig. 9 gives $dq_s/d\chi_s$ due to a trap located at $\chi_s = -6.5$ or about 0.13 ev below the midgap, of density 2.7×10^{11} cm^{-2}, which agrees fairly well with the experimental points after a small continuous density has been superimposed. A higher noise level existed in the measurements of the 17-ohm-cm material, reducing the accuracy near the conductance minimum where the field effect is small, i.e., near $\chi_s = -4$.

Care was taken in all of the runs to maintain a constant flow rate of ambient gas, since a sudden change in flow rate, when the surface was n-type, apparently caused some nonequilibrium process which results in the plot of $\mu_{F.E.}$ *vs* χ_s not retracing the original curve. Increase of flow rate usually caused the non-equilibrium curve to fall below the original curve. This effect is not well understood at present.